Influence of heat treatment on properties of SD251-PH1 composite produced by additive SLM technology

IOP Conf. Series: Materials Science and Engineering **723** (2020) 012003 doi:10.1088/1757-899X/723/1/012003

Influence of heat treatment on properties of SD251-PH1 composite produced by additive SLM technology

[1*]David Bricín, [2]Zdeněk Jansa, [1]Josef Somr, [1]Andrea Elmanová, [1]Antonín Kříž

[1]Department of Material Science and Technology University of West Bohemia in Pilsen. Univerzitni 8 301 00. Pilsen. Czech Republic
[2]New Technologies Research Centre. University of West Bohemia in Pilsen. Univerzitni 8 301 00. Pilsen. Czech Republic

*bricda@kmm.zcu.cz

Abstract. This study evaluates how heat treatment affects the structure and properties of the engineered composite material SD251-PH1. This material was formed by mixing two powder blends in a weight ratio of 90 wt. % WC-Co powder SD251 with 10 wt. % of a PH1 precipitation hardening powder of the stainless steel. Samples were prepared from this mixture on an SLM additive device. The printed samples were then divided into groups. Some of them were left in the initial state and the rest were used for heat treatment based on the standard AMS 5659. Light and electron microscopy metallographic analysis together with X-ray diffraction analysis were then used to evaluate structural and phase changes in the prototype samples. The main attention was paid to changes in the phase composition of the samples. In addition, changes in the size and shape of the pores and tungsten carbide (WC) grains were studied. The metallographic analysis was supplemented by an evaluation of the changes in their mechanical properties and wear resistance. Vickers hardness measurements and the ball on disc test were used for this purpose. The experiments showed that the selected heat treatment processes precipitated new structural phases which differed from the original sample structure in terms of shape, size, chemical composition, and mechanical properties.

Key words: SLM technology. Heat treatment. WC-Co. Porosity. Phase transformation

1 Introduction

The processing of sintered carbides by additive manufacturing, known as SLM (Selective Laser Melting), is a complex process. The processing of this material, as stated in previously published studies [1-7], produces different types of pores [8] and imperfections in the structure, see Figure 1. The volume of these defects in the material structure depends on the parameters used for processing the powder mixture, its residual moisture, the chemical composition of the powder particles, their topography, surface defects and shape.

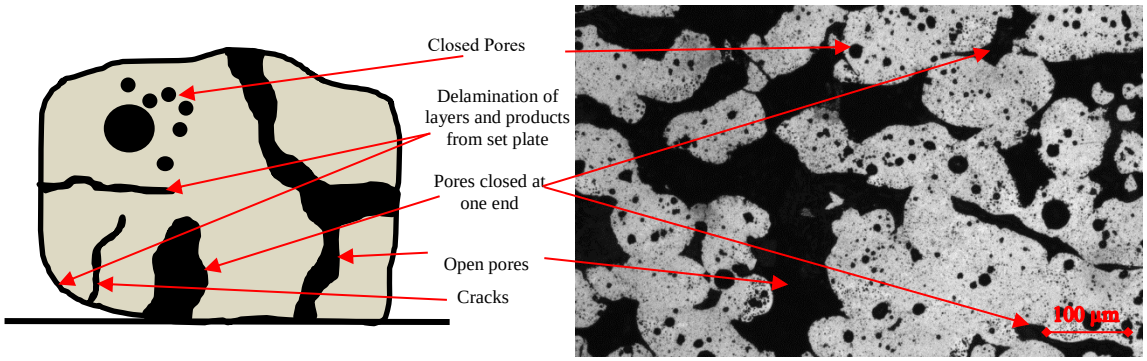

Figure 1. Defects that can be detected in the volume of the builds.

In one previously published study [9], the effect of the SLM process parameters on the properties of the prints made from the SD251 powder blend was evaluated. A high level of porosity and a high degree of delamination of the samples from the set plate was observed in the builds. To reduce the porosity in the builds, WC-Co powder was mixed with PH1precipitation hardening stainless steel powder in this study. One of the aims of this blending was to achieve an increase in the uniformity of the powder layer on the set plate. The unevenness of the powder layer causes changes in the distribution of the temperature field during the interaction of the laser with the powder bed. As a result, different degrees of porosity, different mechanical properties and chemical compositions are observed in different areas of the builds [7, 10]. Furthermore, the addition of secondary powder results in an increase in the proportion of binder in the powder mixture. This should lead, as in the study by R.S. Khmyrov [11], to a crack-free printout structure. Cracks are defects which are very difficult to remove by additional processing. The third reason for adding the steel powder was that precipitates are formed during subsequent heat treatment. All changes which occur during heat treatment could then increase the hardness and abrasion resistance of the formed composite material. This case study aims to assess what structural changes could occur in the composite material thus formed after heat treatment. These changes were evaluated using light microscopy and electron scanning microscopy with EDX analysis of the chemical composition, X-ray analysis of phase composition and analysis of changes in mechanical properties of structural phases using Vickers hardness analysis and analysis of tribological properties by the ball on disc method.

2 Experimental material and processing

2.1 Experimental material

The experimental composite material was formed by mixing two types of powder: SD251 (Figure 2), and PH1 (Figure 3), in a 9:1 weight ratio. The chemical composition of the materials is shown in Table 1. The powder was mixed by mechanical mixing in an unlubricated container for one hour. The aim of this mixing was to obtain a uniform distribution of the PH1 powder in the SD251 matrix. After the powder mixture was prepared, it was processed using an SLM-type additive device. The processing parameters used are summarized in Table 1.

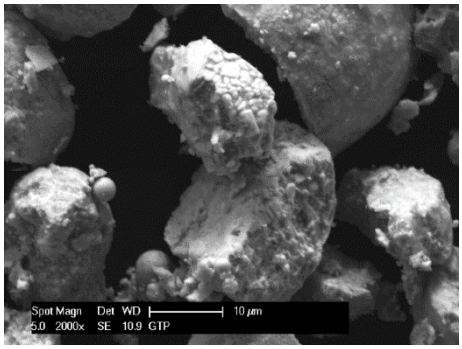

Figure 2. Shape of SD251 powder particles

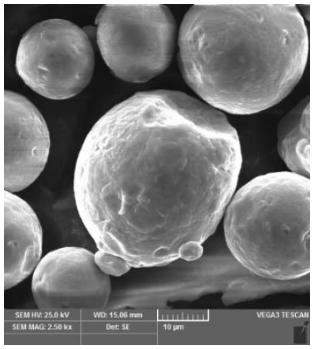

Figure 3. Shape of PH1 powder particles

Table 1. Chemical compositions of powder mixtures and their processing parameters in the SLM additive device.

WC (Wt. %)	Co (Wt. %)	Fe (Wt. %)	Cr (Wt. %)	Ni (Wt. %)	Cu (Wt. %)
87.6±0.61	12.4±0.61	78.6±0.41	14±0.05	3.9±0.23	3.6±0.2
Power of laser (W)	Thickness of powder layer (mm)	Speed of laser spot (mm/s)			Energy density Ev (j/mm3)
250	0.04	900			58

After processing the composite powder on the additive device, the builds were divided into two groups. The first group was left in the state after SLM. The second group was used for heat treatment.

2.2 Method of heat treatment of the experimental material

The heat treatment was carried out according to AMS 5659 Rev. S [12]. It consisted of dissolving annealing, fast cooling, and aging. The dissolving annealing was done to form a homogeneous solid solution in the volume of the prototype samples.

A homogeneous solid solution was not formed in the entire volume of the prototype samples, as is the case with some types of aluminium alloys. This is because the elements from which the composite is composed have different solubilities, with some elements having absolute solubility and some partially limited solubility [13]. The dissolving annealing was followed by rapid cooling at supercritical speed by immersing the samples in water at 20 ° C. This was done to create a supersaturated solid solution in the prototype structure. The last step of the heat treatment was the aging of the samples at elevated temperature. The aim of this step was to form precipitates from the solid solution. The heat treatment parameters used are summarized in Table 2. The heat treatment process was carried out in a single-chamber furnace where the temperature was sensed using a K-type thermocouple which measured with a tolerance of ± 1.5 ^{0}C.

Table 2. Parameters used for the heat treatment of the composite samples. Allowed deviations from the standard times and heat treatment temperatures stated in ASM 5659 are shown in brackets [12].

	Temperature (^{0}C)	Time (min.)	Cooling environment
Dissolving annealing	1038 (±14)	60 (+15)	Water
Variant 482 aging	482 (±9)	60 (+15)	Air
Variant 496 aging	496 (±9)	240 (+30)	Air
Variant 552 aging	552 (±9)	240(+ 30)	Air

2.3 Method of evaluation of prototype samples

Cross sections of all the samples were analysed. This consisted of hot-dipping prototype specimens into a PolyFast moulding material, followed by grinding and polishing on a Tegramin 20 semi-automatic sander. Samples were then analysed using a Philips XL30ESEM electron scanning microscope equipped with an EDX chemical composition analyser. Chemical analysis was done at a magnification of 500x at area of 0,0625 mm^2 at five different locations on each sample.

A CarlZeiss Observer Z1m light microscope and a Panalytical X'pert PRO X-ray diffractometer with a CuKα source of X-ray radiation with a wavelength λKα1 = 0.15405980 nm were used to analyse the structure of the samples. Because the samples are bulk, symmetric geometry was used. With this symmetry were observed the lattice planes (hkl) which are parallel to the sample surface. The planes fulfil Bragg's law ($\lambda=2d\sin\theta$) for each measured 2ϑ angle. XRD patterns were recorded from 30 to 100 degrees in 2ϑ scales. An ultra-fast high-resolution PIXcel detector was used for collecting the diffracted beams. The detection limit for the measurement is about 1 % for each detected phase. The structure of the samples was enhanced by etching using Murakami and Adler etchants. This was supplemented by analysis of the tribological properties using the ball on disc method. Tracks created by the Al_2O_3 ball were than evaluated according to ASTM G99 [14]. Hardness analysis of HV0.05 was also done using a semi-automatic DuraScan hardness tester. Indentations were made at five different places on each sample.

3 Results of experiment and discussion

3.1 Metallographic analysis results

The structure of the builds made of SD251 powder consisted of irregular pores and cracks, see Figure 4 (l). The builds made of composite SD251-PH1 consist of pores with circular and irregular shapes, see Figure 4 (r).

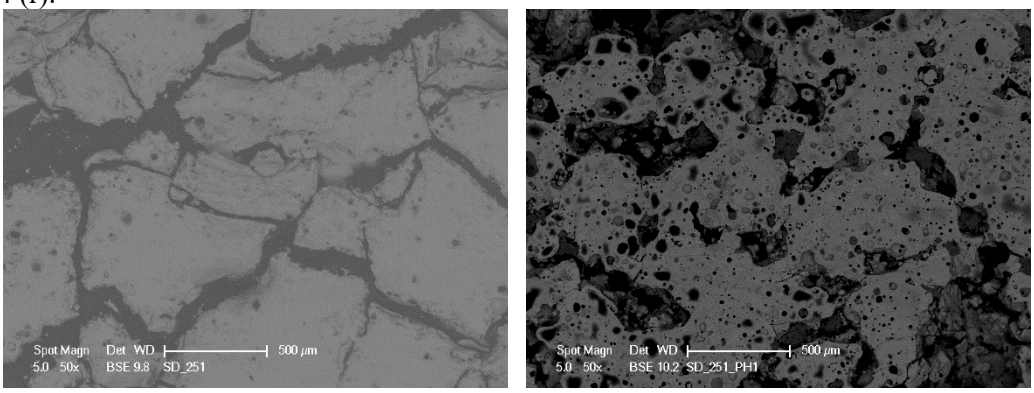

Figure 4. Structure of printed prototype samples. Left image shows build made of SD251 Powder Mixture. Right image shows build made of SD251-PH1 Powder Mixture.

It can be seen from the above that by increasing the proportion of binder by adding steel powder, the development of cracks in the volume of the prototype specimens can be reduced and their degree of delamination reduced.

From the point of view of the proportion of pores in the structure of prototype samples, it was found that the porosity of the samples increased during the heat treatment of the samples. The degree of porosity became higher as the temperature and time of processing increased. In addition to the increase in the porosity, the size of the pores increased and their circularity decreased, see Figure 5.

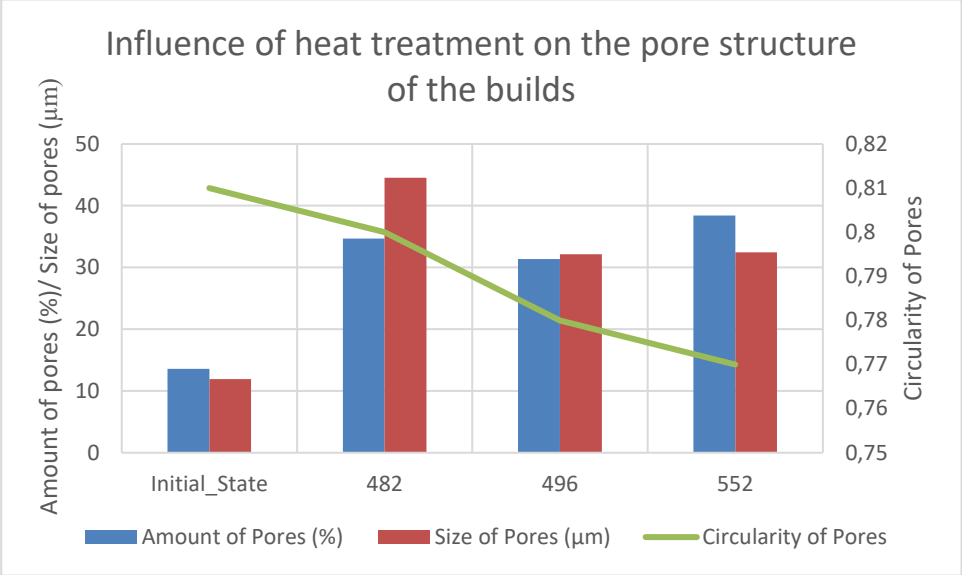

Figure 5. Effect of heat treatment on porosity of builds.

After analysing the porosity of the printed samples, their chemical composition was analysed by EDX element analysis, see Table 3.

Table 3. Comparison of the chemical compositions of builds in the initial state and after heat treatment.

Heat treatment	Cr (Wt. %)	Fe (Wt. %)	Co (Wt. %)	Ni (Wt. %)	Cu (Wt. %)	W (Wt. %)
Initial_state	1.5±0.27	9.8±5.25	8.9±0.62	1.4±0.19	1.4±1	77±6.1
482	2.2±0.23	9.4±0.37	9.2±0.1	1.4±0.14	0.5±0.25	77.4±0.79
496	1.8±0.28	8.6±1.96	9.2±0.2	1.3±0.16	0.7±0.18	78.5±2.15
552	1.9±0.52	9.8±1.84	9.7±0.65	1.6±0.16	1.1±0.38	76±3.3

It can be seen from the table above that there were no significant changes in chemical composition during heat treatment.
However, the metallographic analysis showed structural changes induced by thermal processing, see Figures 6-9 below. It can be seen that the initial triangular to rectangular shapes of the WC grains turn to cigar shaped structures after heat treatment.

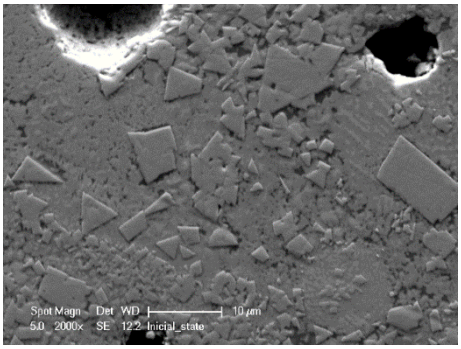

Figure 6. Build structure in original state without heat treatment. Magnification 2000x.

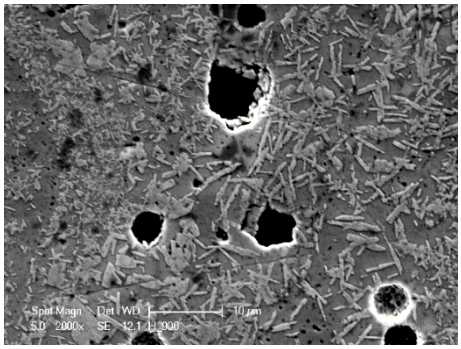

Figure 7. Build structure after Variant_482 heat treatment. Magnification 2000x.

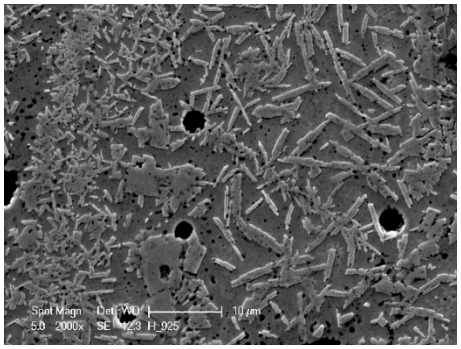

Figure 8. Build structure after Variant_496 heat treatment. Magnification 2000x.

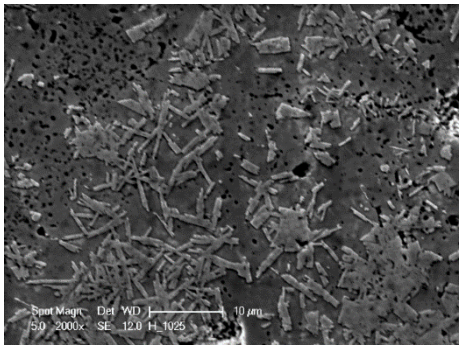

Figure 9. Build structure after Variant_552 heat treatment. Magnification 2000x.

Coarsening of the precipitated grains of WC can be seen in the images above. This change occurs due to the increasing temperature of the aging process. The metallographic analysis was supplemented by a hardness analysis of the observed structural phases, see Table 4.

Table 4. Average values of microhardness HV0.05 of the structural phases of the builds.

Heat Treatment	Average hardness of WC grains	Average hardness of matrix	Average hardness of precipitate phase
Initial State	1860±270	1277±285	-
Variant_482	822±380	1089±165	1016±170
Variant_496	1221±283	947±112	1506±169
Variant_552	1088±57	649±125	1340±185

The results from the hardness measurements show that the newly precipitated phase probably has a changed coherence of its lattice due to the diffusion-activated displacement of atoms during the heat treatment of the builds. The process of diffusion, especially of interstitial elements, also influences the final hardness of the carbide phase and the matrix of the builds, when concentration gradients are gradually balanced in the volume of the evaluated samples.

3.2 X-ray diffraction analysis results

X-ray diffraction analysis confirmed changes in the phase composition of samples before and after heat treatment, see Figure 10.

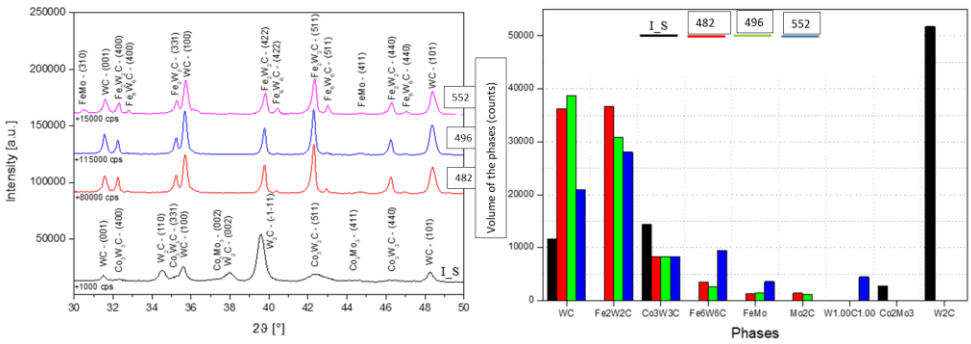

Figure 10. X-ray diffraction analysis and calculated volume fraction of phases in prototype samples.

From the graph above (Figure 11), it can be seen that the initial structure of the builds consisted of the WC, W2C, Co2Mo3, Co3W3C and the Fe-C phase. The Fe-C phase cannot be seen in the image due to its low peak intensity. Therefore it was not possible to count its right volume for the initial state builds. After heat treatment, the structural phases of WC, Fe_2W_2C, Fe_6W_6C, Co_3W_3C, FeMo and Mo_2C were recorded in the volume of the builds.
The difference in the volumes of the phases occurred due to the diffusion flow of the interstitial and substitution elements in the volume of the builds. Diffusion of the carbon especially affected the amount and type of phases in the volume of the builds after their aging.
The less stable phase of W2C decayed. The released carbon then interacted with other elements to form new structural phases, see Figure 11.

3.3 Tribological properties

The aim of this analysis was to assess the effect of the structural changes on the frictional properties of the heat treated builds. The results in Figure 11 show that the heat treatment reduces the wear rate.

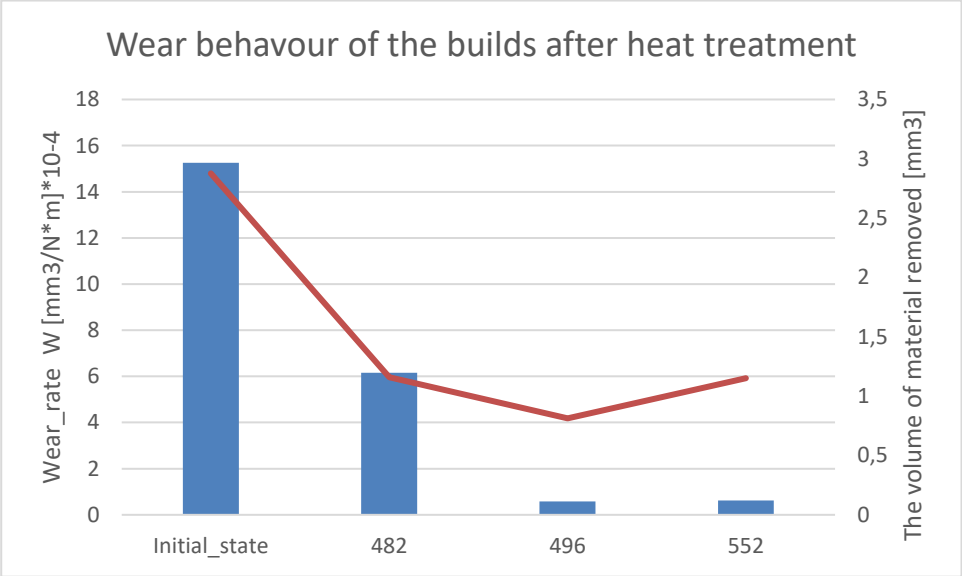

Figure 11. Analysis of tribological properties of builds before and after heat treatment.

These results also show a re-increase in the degree of wear of the samples which were aged according to variant C of the used aging process.. This is probably associated with the recorded increase in the volume and size of the pores detected in the volume of the prints after heat treatment.

4 Conclusion

Heat treatment of builds made from composite material SD251-PH1 had a relatively high effect on the homogeneity of the material structure. This was confirmed by X-ray diffraction analysis, metallographic analysys and subsequent ball on disc tribological testing, where the heat treated samples have lower wear rates than the builds without heat treatment.

During heat treatment, the development of newly precipitating phases was recorded by metallographic analysis, and was subsequently confirmed by X-ray diffraction analysis. The newly detected phases included Fe_2W_2C, Fe_6W_6C, FeMo, and Mo_2C. They were not detected in the heat treated prints due to the diffusion phenomena of the W2C phase, which was transformed into a WC phase. Heat treatment had a negative impact on the development of the porosity of the builds. Porosity increased by up to 24 percent compared to builds without heat treatment. This phenomenon occurred in samples that were aged at the highest temperature. In addition to their volumetric increase, the pores changed shape, with a gradual decrease in their circularity, which in turn has a

negative impact on the fracture toughness of the material. In addition, the newly precipitating structural phases gradually coarsened and the coherence of the lattices of the precipitates changed. This was confirmed by measuring a micro-hardness of HV0.05 for the original structural phases and precipitates.

The highly porous material thus prepared can be used in the future as a filter material for liquid particulate media. However, for its possible application, it is necessary to conduct further experiments aimed at evaluating its utility properties.

Next research will also focus on looking for other alternative composite powder blends for SLM processes and other additive techniques. This new research will evaluate the quality of feedstocks and also the influence of the parameters of the manufacturing process on the properties of the final builds, focusing on mechanical behaviour, chemical composition changes and phase changes.

Acknowledgments

This work was supported by CEDAMNF project (CZ.02.1.01/0.0/0.0/15_003/0000358), co-funded by the ERDF as part of the OP RDE programme of the Ministry of Education, Youth and Sports (Czech Republic) and by the project Zéta TJ01000218 'Production of a machine tool using additive SLM technology' of TAČR, Technology Agency of the Czech Republic. The build used in this study was made in cooperation with the Technical University of Liberec, the Institute for Nanomaterials and New Technologies and New Technologies Research Centre at the University of West Bohemia in Pilsen.

References

[1] Uhlmann E Bergmann A and Gridin W 2015 Investigation on Additive Manufacturing of Tungsten Carbide-cobalt by Selective Laser Melting *Proc. CIRP* 35 pp 8-15.

[2] Domashenkov A Borbély A and Smurov I 2016 Structural modifications of WC/Co nanophased and conventional powders processed by selective laser melting *Mat. and Man. Proc.* DOI: 10.1080/10426914.2016.1176195 ISSN 1042-6914 Aviable from: https://www.tandfonline.com/doi/full/10.1080/10426914.2016.1176195

[3] Kumar S 2009 Manufacturing of WC–Co moulds using SLS machine *J. of Material Processing Tech.* DOI: 10.1016/j.jmatprotec.2008.08.037 Aviable from: http://linkinghub.elsevier.com/retrieve/pii/S0924013608006705

[4] Gu D Shen Y Dai P and Yang M 2006 Microstructure and property of sub-micro WC-10 %Co particulate reinforced Cu matrix composites prepared by selective laser sintering DOI: 10.1016/S1003-6326(06)60061-7 Aviable from: http://linkinghub.elsevier.com/retrieve/pii/S1003632606600617

[5] Gu D and Meiners W 2010 Microstructure characteristics and formation mechanisms of in situ WC cemented carbide based hardmetals prepared by Selective Laser Melting *Mat. Scien. and Eng.* DOI: 10.1016/j.msea.2010.08.075 Aviable from http://linkinghub.elsevier.com/retrieve/pii/S092150931000986X

[6] Kumar S and Czekanski A 2017 Optimization of parameters for SLS of WC-Co *Rap. Prot. J.* DOI: 10.1108/RPJ-10-2016-0168. Aviable from: http://www.emeraldinsight.com/doi/10.1108/RPJ-10-2016-0168

[7] Bricín D Špirit Z and Kříž A 2018 Metallographic Analysis of the Suitability of a WC-Co Powder Blend for Selective Laser Melting Technology DOI: 10.4028/www.scientific.net/MSF.919.3. Dostupné z: https://www.scientific.net/MSF.919.3

[8] Zdravkov B Čermák J Šebera M and Janků 2007 Pore classification in the characterization of porous materials: A perspective *O. Chem.* DOI: 10.2478/s11532-007-0017-9 ISSN 2391-5420. Aviable from: http://www.degruyter.com/view/j/chem.2007.5.issue-2/s11532-007-0017-9/s11532-007-0017-9.xml

[9] Bricín D Elmanová A and Kříž A 2019 The effect of selective laser melting technology on the Development of the structure of samples made from WC-Co powder *Mat., met. and tech. conf. 2019*

[10] Bricín D and Kříž A 2019 Processability of WC-Co powder mixtures using SLM additive technology *MM Sc. J.* DOI: 10.17973/MMSJ.2019_06_2018115 Aviable from: http://www.mmscience.eu/2018115
[11] Khmyrov R S Safronov V A and Gusarov A V 2016 Obtaining Crack-free WC-Co Alloys by Selective Laser Melting *Phys. Proc.* DOI: 10.1016/j.phpro.2016.08.091. Aviable from http://linkinghub.elsevier.com/retrieve/pii/S1875389216301985
[12] AMS 5659 2019 Available from: https://www.aksteel.com/sites/default/files/2018-11/15-5-ph-stainless.pdf [Accessed 22 Jul. 2019]. Rev. S *: Heat Treatment of Steel Raw Materials - SAE International*. ASM 5659
[13] Baker H 1999 Alloy phase diagrams *ASM Int.* Materials Park Ohio
[14] ASTM G99 2016 Standard Test Method for Wear Testing with a Pin-on-Disk Apparatus. [online] *Astm.org*. Available at: https://www.astm.org/DATABASE.CART/HISTORICAL/G99-05R16.htm [Accessed 28 Aug. 2019].